

# Investigation of the performance of a stand-alone horizontal axis tidal current turbine based on in situ experiment



Quankun Xu, Wei Li, Yonggang Lin\*, Hongwei Liu, Yajing Gu

State Key Laboratory of Fluid Power and Mechatronic Systems, Zhejiang University, Hangzhou 310027, China

## ARTICLE INFO

### Article history:

Received 13 October 2014

Accepted 27 December 2015

### Keywords:

Stand-alone HATCT

In situ experiment

MPPT

Power limitation

Rotor performance

## ABSTRACT

To investigate the performance of a stand-alone horizontal axis tidal current turbine (HATCT) under an actual tidal current, a stand-alone HATCT, including its rotor, power train, electrical system, control system and support structure, was designed, and in situ experiments for a whole rising tide period were carried out in a water channel in Zhoushan, China. The experimental results show that the turbine that was designed had a good starting characteristic that began generating at a tidal current velocity of 0.588 m/s. Both the MPPT control strategy to capture maximum power under the rated tidal current velocity and the power limitation control strategy to limit output power above the rated tidal current velocity were verified.

© 2016 Published by Elsevier Ltd.

## 1. Introduction

Many renewable energy resources are being exploited to reduce the dependence on fossil fuels and carbon emissions. Tidal current energy has advantages, such as regularity, predictability and high density, over other renewable energy resources (Bahaj and Myers, 2003), which makes large scale utilization possible. In recent years, various devices have been developed to harvest tidal current energy, among which the horizontal axis tidal current turbine (HATCT) is considered to be one of the most promising, thus making the HATCT more and more popular with tidal energy developers (Ng et al., 2013; Roc et al., 2014; Val et al., 2014). For some remote islands, where it is difficult to connect to a power grid, the HATCT offers an alternative to solve the problem of electricity shortage because of its feasibility and removability. Methods to study the performance of the HATCT fall into two categories: numerical simulation and practical experiment. Conducting a numerical simulation is an economical and convenient way to predict the performance of the HATCT, but to understand exactly how the HATCT operates in an actual marine environment, conducting an experiment is essential. Gaurier et al. (2013) conducted a flume tank experiment to study the characteristics of a marine current turbine with ocean currents and wave loading. Batten et al. (2007) performed tunnel experiments to validate the hydrodynamic design of the HATCT. Bahaj et al. (2007) discussed the hydrodynamic performance of a HATCT using flume tunnel experiments. However, these

experiments were all conducted in a laboratory, and the conditions of the experiments were idealized and controllable. SeaGen (Chick et al., 2008; MacEnri et al., 2011), a grid-connected HATCT developed by Marnie Current Turbine, Ltd., was installed in Strangford Lough, Northern Ireland, and started power production in May 2009. Because of commercial secrecy, the design details of the turbine and in-field experimental data were rarely published.

The objective of the present paper is to report the study of the performance of a designed stand-alone HATCT in an in-field experiment conducted in a tidal current channel between two islands. The experimental results were compared with theoretical predictions to verify the design of the turbine rotor, control strategy and entire power conversion system. This in situ experiment lends empirical support to the operation of the single stand-alone HATCT and the microgrid of the HATCT array.

## 2. Experimental methods

### 2.1. Tidal current turbine

The turbine tested in this experiment is a horizontal axis tidal turbine that is composed of a three-blade rotor, a semi-direct drive gearbox, a permanent magnet synchronous generator (PMSG), and an electricity conversion system installed above sea water. The tidal current turbine configuration is shown in Fig. 1.

#### 2.1.1. Turbine rotor design

The rated power of the rotor is 60 kW, and the rated current velocity is set to 2 m/s after a marine survey was conducted at the

\* Correspondence to: The State Key Laboratory of Fluid Power Transmission and Control, Zhejiang University, Hangzhou 310027, China. Tel./fax: +86 571 85876950.  
E-mail address: [yglin@zju.edu.cn](mailto:yglin@zju.edu.cn) (Y. Lin).

## Nomenclature

$N_1/N_2$	rotating speed of gearbox input/output shaft
$P_{\text{rated}}$	rated power of the rotor, kW
$\rho$	density of sea water, kg/m <sup>3</sup>
$v$	tidal current velocity, m/s
$R$	radius of the turbine rotor, m
$C_P$	rotor power efficiency
$C_{P_{\text{rated}}}$	rated rotor power efficiency
$C^*$	desired rotor power efficiency
$n_{\text{rated}}$	rated rotating speed of the rotor, rpm
$\lambda$	tip speed ratio (TSR)
$\lambda_{\text{opt}}$	optimal tip speed ratio
$\lambda^*$	desired tip speed ratio
$v_{\text{rated}}$	rated tidal current velocity, m/s
$D$	diameter of the rotor, m
$C_L/C_D$	lift/drag coefficient

$\sigma$	cavitation number
$P_{\text{AT}}$	atmospheric pressure, Pa
$P_V$	vapor pressure of sea water at 25 °C, Pa
$h$	hub depth of the turbine, m
$V$	local tidal current velocity, m/s
$r$	local blade element radius in turbine rotor, m
$c$	chord length of blade element, m
$t$	thickness of blade element, m
$\text{Twist}$	twist angle of blade element, degree
$\omega_{\text{opt}}$	optimal rotating speed of the PMSG, rad/s
$\omega_f$	feedback rotating speed of the PMSG, rad/s
$\omega^*$	desired rotating speed of the PMSG, rad/s
$P_{\text{lim}}$	limitation power, kW
$i$	speed-up ratio of the gearbox
$P_{\text{rotor}}$	power captured by the turbine rotor, kW
$P_{\text{gen}}$	output power of the PMSG, kW
$\eta_{\text{gb}}/\eta_{\text{gen}}$	efficiency of the gearbox/PMSG

experimental sea site, which will be discussed in detail in Section 2.2. To estimate the output power of the rotor, the power efficiency was substituted into Eq. (1):

$$P_{\text{rated}} = \frac{1}{2} \rho v^3 \pi R^2 C_{P_{\text{rated}}} \quad (1)$$

where  $P_{\text{rated}}$  is the rated power of the rotor,  $\rho$  is the density of sea water,  $v$  is the tidal current velocity,  $R$  is the radius of the turbine rotor, and  $C_{P_{\text{rated}}}$  is rated rotor power efficiency.

$C_P$  varies versus the tip speed ratio (TSR)  $\lambda$ . When  $\lambda_{\text{opt}}$  is given, the rated rotating speed of the rotor can be calculated by Eq. (2):

$$n_{\text{rated}} = \frac{\lambda_{\text{opt}} v_{\text{rated}}}{D} \cdot \frac{60}{\pi} \quad (2)$$

where  $n_{\text{rated}}$  is the rated rotating speed of the rotor,  $\lambda_{\text{opt}}$  is the optimal tip speed ratio, and  $D$  is the diameter of the rotor.  $v_{\text{rated}}$  is the rated tidal current velocity. Table 1 shows the fundamental design parameters for the rotor that was designed.

The hydrodynamic characteristics are very important in the selection of a high performance hydrofoil (Singh and Choi, 2014). The performance of the turbine depends on three very important parameters: the lift coefficient ( $C_L$ ), lift to drag ratio ( $C_L/C_D$ ), and Reynolds number. These three parameters vary with respect to the angle of attack (AOA). The design objective of the blade is to keep every section of the blade at the optimal AOA at which  $C_L/C_D$  has a maximum value, while keeping the value of  $C_L$  considerably high. The blades used in this rotor are developed from the profile shape of a NACA 634xx series and along with the chord, thickness and twist distribution are presented in Table 2, with an optimal AOA of

approximately 6°. The blade strength is also very important in the HATCT, as the blades have to withstand a huge thrust force as a result of the high density of sea water. For this reason, the hydrofoils need to be thick compared to the airfoils. Thicker hydrofoils mean a loss in  $C_L/C_D$  as well as poor performance, and vice versa. A solution to this problem is to make the blade thick near the root to withstand the thrust, and hydrofoils from the mid-section to the tip are slightly thinner for better performance (Goundar and Ahmed, 2014). Table 2 shows that the thicknesses of the chosen hydrofoils decrease linearly from the root to the tip.

Cavitation is a crucial design constraint that causes structural damage to the turbine blades and decreases the performance by decreasing the  $C_L/C_D$  ratio (Goundar and Ahmed, 2013). The cavitation model is based on the assumption that the water and vapor

**Table 1**  
Rotor design parameters.

Design parameters	Values
$P_{\text{rated}}$	60 kW
$v_{\text{rated}}$	2 m/s
$C_{P_{\text{rated}}}$	0.4
$N$	3
$D$	7.5 m
$n_{\text{rated}}$	36 rpm
$\lambda_{\text{opt}}$	7.0
$\rho$	1025 kg/m <sup>3</sup>

**Table 2**  
Particulars of the turbine blade geometry.

$r/R$	$c$ (m)	$t$ (m)	Twist (deg)	$t/c$ (%)
0.125	0.19	0.19	0	100
0.1875	0.19	0.19	0	100
0.25	0.325	0.1625	0	50
0.3125	0.46	0.1288	16	28
0.375	0.41	0.1066	12.5	26
0.4375	0.37	0.0925	10	25
0.5	0.337	0.08088	8	24
0.5625	0.306	0.07344	6.28	24
0.625	0.288	0.06336	4.8	22
0.6875	0.263	0.05786	3.8	22
0.75	0.24	0.0528	2.9	22
0.8125	0.215	0.0473	2	22
0.875	0.19	0.0418	1.2	22
0.9375	0.164	0.0328	0.5	20
1	0.14	0.0252	0	18

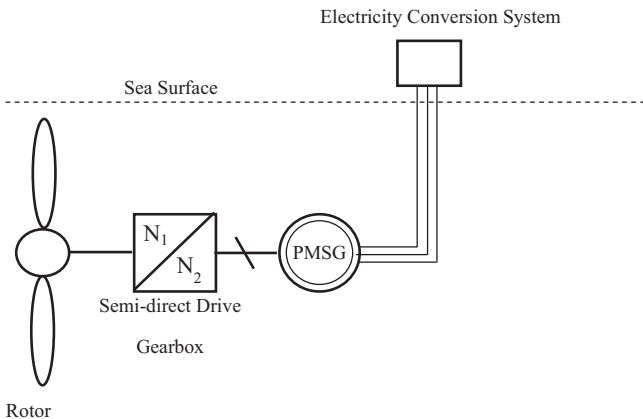


**Fig. 1.** Tidal current turbine configuration.

Download English Version:

<https://daneshyari.com/en/article/8064834>

Download Persian Version:

<https://daneshyari.com/article/8064834>

[Daneshyari.com](https://daneshyari.com)